© JUL 2025 | IRE Journals | Volume 9 Issue 1 | ISSN: 2456-8880

Evaluation of the Corrosion Inhibition Performance of Orange Leaf Extract on Aluminium in Basic Media

IBIAM PRINCE AMAUCHE[1], ABOJE VIVIAN AJENU[2], ILEABOYA EMMANUEL EROMOSEI[3], OKAFOR BLESSING ONYINYE[4]

[1, 2, 3, 4]Gregory University Uturu, Abia state, College of Engineering, Department of Chemical Engineering

Abstract- ***In this study, gravimetric and electrochemical techniques were employed to investigate the effects of orange leaf extract (OLE) on the inhibition of aluminum corrosion in alkaline environments. The material was characterized using Fourier Transform Infrared Spectroscopy (FTIR), while surface morphology was examined using Electron Dispersive X-ray Spectroscopy (EDX) and Scanning Electron Microscopy (SEM). Additionally, Potentiodynamic Polarization (PDP), Electrochemical Impedance Spectroscopy (EIS), and Open Circuit Potential (OCP) were utilized to analyze the corrosion inhibition process. The results of the study indicate that the extract displays significant effectiveness in preventing the corrosion of aluminum under basic conditions, exhibiting inhibition efficiencies of 90% at 303 K and 84.85% at 313 K. It was observed that the inhibitory efficiency of the extract decreased with higher temperatures and longer immersion times, while it increased with higher concentrations of the extract. These findings suggest that the extract has potential as a corrosion inhibitor for aluminum in basic environments. The inhibition observed in the study can be attributed to the adherence of inhibitor molecules to the surface of the aluminum sample, as outlined by the Temkin adsorption isotherm. It was found that the functional groups O-H and N-H were primarily responsible for the inhibitory effects of the extracts. Additionally, the results of the potentiodynamic polarization (PDP) indicated that orange leaf extract (OLE) functions as a mixed-type inhibitor. SEM investigations confirmed the formation of a protective coating on the metal surface, leading to a reduced rate of corrosion. Furthermore, the hydrophobic nature of aluminum in the presence of the inhibitor was demonstrated. Overall, the findings suggest that orange leaf extract is effective as a corrosion inhibitor for aluminum in basic media.***

Indexed Terms- Evaluation, Corrosion, Inhibition Performance, Orange Leaf Extract, Aluminum, Basic Media

I. INTRODUCTION

The depletion of valuable resources such as iron, aluminum, copper, chromium, manganese, and titanium is a pressing concern for nations. The imminent scarcity of these metals is a looming reality that must be addressed. Understanding the destructive impact of corrosion on these essential materials and the potential of corrosion protection technology to mitigate this issue is crucial for conservation efforts. Aluminum, in particular, holds significant economic importance across various industries, yet it is highly susceptible to corrosion in harsh environmental conditions, which may consist of liquids, gases, or mixtures. Corrosion, a natural deterioration process caused by the reaction of materials with their surroundings, is not limited to metals but also affects other substances [1]. Corrosion not only decreases an object's usefulness and lifespan but also poses serious safety and economic repercussions through structural damage. Electrochemical corrosion is the most common type, involving electron transfer across a metal surface, requiring an electrolyte like water or moisture and an electrochemical cell with an anode and a cathode.

The process of corrosion in industries, such as oil and natural gas pipelines and industrial plant construction, is primarily driven by the metal oxidation process. This involves the production of metal ions at the anode, while a different species, typically oxygen or hydrogen ions, are reduced at the cathode [2]. Given the importance of this process, protecting metals with alternative corrosion inhibitors. As a result, there is increasing exploration of natural organic inhibitors derived from plant extracts, which contain phytochemical components. These inhibitors are being considered as safer and eco-friendly options to form protective layers on metal surfaces, thereby inhibiting the oxidation and reduction phases of the redox reaction [3,4].

Therefore, in the current investigation, non-electrochemical methods were employed to assess the inhibitory characteristics of leaf extract from *Citrus sinensis* on aluminum metal. The suppression of corrosion will be investigated using the alcoholic basis of *Citrus sinensis* leaf extract. Because of its mechanical strength and resilience, aluminum is typically used to make gas cylinders and gas-transporting automobiles, although metal is also prone to corrosion. [5]. The main detrimental impacts of corrosion include diminished mechanical strength, structural failure or damage, loss of product value, and fluid contamination in pipes and containers. Metallic degradation is one of the key elements affecting a system's dependability in the transportation, oil, gas, chemical, and automotive industries [6]. For example, thousands of kilometers of pipelines, pumps, pressure vessels, and storage vessels are used in the oil, gas, and petrochemical sectors for the processing, storing, and transportation of various goods. These infrastructures indirectly support the national economy and are essential to the continuation of these sectors. Unfortunately, the majority of these installations and the parts that make them up are composed of aluminum, which means that they will eventually corrode or deteriorate. [7]. Most of the time, these mistakes could lead to product spills, which are always bad for society since they put people's safety at danger, the environment at risk, and there's a significant financial and time loss associated with production. Furthermore, since compensation and legal action may be involved, this kind of publicity is intolerable. Thus, a great deal of focus is placed on the observation and examining these establishments. The exceptional qualities of aluminum, like its easy availability, high strength, and durability, make it a popular metal in industries. In order to handle different corrosive liquids and create different aggressive solutions, such acidic, basic, and salt solutions, it is mostly utilized in the building of reaction vessels and tanks. In many petrochemical processes, basic solutions are also utilized for basic cleaning, the production of basic chemicals and polymers, and more. Hydrogen sulfide and mercaptans are extracted from a variety of hydrocarbons using sodium hydroxide solutions in petroleum refining. [8]. The most fundamental solutions are used to produce organic compounds, with epoxypropane a crucial ingredient in the production of polyurethanes being one of the most significant. Additionally, a lot of oil exploration, production, and descaling activities use these fundamental solutions for drilling, hydraulic fracturing, and basic simulations.

Aluminum is easily corroded by basic environments because they can target the metal's surface through an interfacial reaction that dissolves the metal and releases ions, which can occur in a variety of industrial processes. Aluminum is more prone to attack than its oxide when exposed to alkaline conditions, leading to corrosion and faster attack in the event of a localized perforation in the aluminum oxide film. Aluminum dissolves more quickly in bases than in acids. Metal pitting, a severe kind of corrosion, happens when aluminum is subjected to extremely strong alkaline environments outside of the pH range of 4 to 9. [9].

According to [10], corrosion is a naturally occurring electrochemical phenomena brought on by the potential difference between acid and metal. We refer to dissolved oxygen and hydrogen ions as the "natural motors of corrosion." Corrosion needs to be contained as cheaply as feasible in order to optimize earnings. Numerous substances have been identified as agents that induce corrosion, and a comprehensive grasp of the causes of corrosion will be necessary for effective, economical management [11]. Among these agents are CO2, water, and acid-base combinations. When water gets inside a pipeline while transporting crude oil, corrosion happens. Drilling produces water with the product, which adds to the corrosion. Consequently, CO_2 and H_2O attack pipelines. Bacteria also attack them when microbial induced corrosion (MIC) occurs. There are also the impacts of H_2S and sand. Separators, valves, and vessel tanks are examples of other fixed mechanical support equipment used in the oil and gas industry that is prone to different forms of corrosion. This suggests that an effective and economical method of controlling corrosion would involve optimization and reliability checks [12].

Nonetheless, finding answers to issues related to metal deterioration from corrosion especially aluminum has grown in importance. The expensive replacement costs of damaged metals, which are brought on by corrosion, can be reduced by the application of corrosion inhibitors. [13]. The best way to prevent metal from corroding is to use corrosion inhibitors in industries and other fields. When added in the right amounts, these inhibitors can lower the rate at which metal corrodes without appreciably altering the concentration of other agents. Corrosion is an unstoppable process. [14]. These are also compounds that, in modest doses, improve the resistance of an electrochemical system to environmental corrosive agents or corrosion itself.

Industrial uses of corrosion mitigation solutions are common, especially in the extraction and refinement of crude oil, water treatment, circulation and cooling infrastructures, and various manufacturing processes, such as solution baths and transport. It can be challenging to understand inhibitor compounds' intricate interactions with electrochemical systems because they can be either organic or inorganic and are frequently proprietary [15].

Mechanistic characterization can be carried out using surface characterization methods and other electrochemical tests. In order to ascertain if inhibitor compounds can interact with corrosion products such metal ions, metal oxides, or other dissolved species, several researchers have also looked at the compositions of electrolytes. [16]. Investigative techniques like this might reveal secondary inhibition mechanisms that shed light on why inhibitors with comparable chemical structures work markedly differently as inhibitors or explain synergistic effects. The primary material used to build cisterns in the oil and gas industry that store crude oil until use, also referred to as hold-up tanks is aluminum. This is a significant process in the petroleum sector overall. Furthermore, even in processing plants, aluminum pipes are used for the mechanical and budgetary benefits of transporting crude oil. [17]. Additionally, fittings (valves, actuators, and strainers) composed of aluminum alloys and, in certain case, other metallic alloys are attached to these pipes. But with time, they become susceptible to the negative effects of crude oil since they come into contact with it so often. Sulfuric acid will invariably cause varying degrees of corrosion to the metal substrate when used for pickling, etching, descaling, and cleaning metal surfaces. [18]. Most basic solutions aggressively attack aluminum; sodium carbonate solutions also attack metal; aluminum equipment handles a lot of sodium chloride, both in solid and in solution; and sodium hydroxide (NaOH) solution dissolves aluminum easily. The detrimental consequences become evident when the effective diameter or thickness caused by metal loss from corrosive assault reduces the facility's ability to support loads, such as shafts or shell thickness. It is imperative to maintain these metallic structures because their effective diameter or thickness cannot withstand the tensile, compressive, or radial loads. Failure becomes immediate and occasionally catastrophic. Numerous organic compounds with heteroatoms including O, S, and N have been shown to be efficient corrosion inhibitors; yet, the majority of these compounds are highly expensive, harmful to human health, and contaminate the environment. Among corrosion inhibitors, natural products are unique due to their high efficiency, affordability, availability, and environmental friendliness. [19]. Research on corrosion inhibitors based on biological products and extremely acidic and basic substances has dominated the field thus far; very few studies have looked at plant extracts. The majority of study has been on the usage of ordinary metals like iron and mild steel in acidic environments. [20]. This study was necessary to close a knowledge gap because there was little literature on the utilization of organic materials from plant products as an aluminum corrosion inhibitor in basic media.

II. METHODOLOGY

2.1 Materials

The equipment list is shown in Table 1 and Table 2 lists the chemicals and reagents used in this investigation. The compounds were all analytical grade, with a purity percentage ranging from 95 to

99.9%. They were all utilized exactly as supplied, requiring no additional purification.

Table 1: Chemicals and Reagents

Material	Manufacturer	Purity (%)
H_2SO_4	England's BDH	98.0
HCl	England's BDH	98.0
NaOH	England's BDH	97.0
Soduim hydroxide	England's BDH	99.0
Ferric Chloride	England's BDH	99.0
Copper sulphate	England's BDH	98.0
Ethanol	England's BDH	99.0
Acetone	England's BDH	99.0
Acetic anhydride	England's BDH	98.0
Mayer's Reagent	England's BDH	97.0
Distilled Water	-	-
Orange Leaves	Okada, Nigeria	-

Table 2: Equipment/Apparatus

Instrument	Manufacturer	Model
Electric	Gallenkamp,	PI09334
Electronic	Ohaus	Scout Pro
Beakers	England	Pyrex
Volumetric	England	Pyrex
Whatman filter	Whatman	110mm
Masking tape	-	-
Scientific	Perkin Elmer	M530
Scanning	Eindhoven,	MVE01647
Mild steel	Nigeria	-
Plastic thread	Nigeria	-
Potentiostat/gal	Netherland	Autolab
Spatula	-	-
Funnel	-	-
Sieve	Interlab, Seithi	ASTM No
Magnetic	Gallenkamp,	78HW-1

2.2 Materials collection and preparation

2.2.1 Preparation of aluminum sample

The aluminum was mechanically chopped into 3 × 3 mm coupons in preparation for the gravimetric examination. Using plastic thread, a tiny hole was created at one end of the coupons to enable their suspension in the test solution. The aluminum specimen for the electrochemical investigations was trimmed to a 10 × 10 mm size. Using silicon carbide emery paper of various grades (400 to 1200 grit), the mechanically abraded coupons' surfaces were prepared. They were then cleaned with acetone, rinsed with distilled water, and kept in a desiccator until needed.

2.2.2 Base preparation

In order to create a corrosive environment, 28 mL of 98% NaOH (Merck) stock were diluted with distilled water and added to a 1 L standard flask to create a 0.5 M NaOH solution.

2.2.3 Preparation of OLE

Orange leaves were gathered from a garden in Okada, Nigeria's Edo State. The leaves were pounded into a powder after being dried for seven days out of the sun. First, 100 g of the powdered leaf were weighed and incubated for 48 hours in a 500 mL beaker of ethanol. The extract was filtered through Whatman filter paper (grade 1) after it was evaporated using a rotary evaporator. Three different concentrations of 0.3, 0.6, and 0.9 g/L were used to prepare the extract.

Figure 1: Okada Edo state

2.2.4 Examining the extracts phytochemically

The extracts were screened phytochemically using reagents including Meyer's, aqueous NaOH, acetic anhydride, 1% $FeCl_3$, and copper sulphate solution to find secondary metabolites such alkaloids, flavonoids, tannins, saponin, and protein.

2.2.5 Flavonoids determination

At room temperature, 100ml of 80% aqueous methanol was used to extract 5g of the material many times. Whatman filter paper No. 4, measuring 125 mm, was used to filter the entire mixture. Following its transfer into a crucible, the filtrate was dried over a water-bath at 80˚C and weighed to ensure a consistent weight [20].

$$\% \, Flavonoids = \frac{\text{(weight of crucible +residue)} - \text{(weight of crucible)}}{\text{Weight of sample analyzed}} \times 100$$

2.2.6. Alkaloid determination

A 250 ml beaker containing 5 g of the sample was filled with 200 ml of 20% acetic acid in ethanol, capped, and left to stand at 250˚C for 4 hours. This was filtered through No. 4 filter paper, and the filtrate was concentrated to a quarter of its initial volume in a water bath. Up until the precipitation was fully formed, concentrated ammonium hydroxide was added to the extract drop by drop. After letting the entire mixture settle, the precipitate was gathered and cleaned with diluted NH_4OH (1% ammonia solution). Next, use pre-weighed filter paper to filter. After being dried at 80˚C in the oven, the residue on the filter paper is weighed [21, 23].

Calculation:

$$\% \, Weight \; of \; Alkaloid = \frac{\text{weight of filter paper with residue} - \text{weight of filter paper}}{\text{Weight of sample analyzed}} \times 100$$

2.2.7 Tannin determination

100ml of petroleum ether was added to 5g of the crushed material in a conical flask, which was then sealed for a full day. Following filtering, the sample was let to stand for 15 minutes so that the petroleum ether may evaporate. It was then re-extracted by soaking it for four hours in 100 milliliters of 10% acetic acid in ethanol. After then, the sample was filtered, and the filtrate was gathered. To precipitate the alkaloids, the filtrate was mixed with 25 milliliters of NH_4OH. To get rid of part of the NH_4OH that was still in solution, the alkaloids were heated on an electric hot plate. Thirty-three milliliters was the volume left. We took 5 ml of this and mixed it with 20 ml of ethanol. Phenolphthalein was used as an indicator while titrating it with 0.1M NaOH till a pink end point is reached. [21].

2.2.8 Saponin determination

After 5g of the material was weighed into a flask with 20% acetic acid in ethanol, it was left to stand for 24 hours at 500˚C in a water bath. This was filtered, and a water bath was used to concentrate the extract to a quarter of its initial volume. [22]. Drop by drop, concentrated NH_4OH was added to the extract until the precipitate was fully formed. After letting the entire mixture settle, the precipitate was filtered out and weighed. A percentage was computed by weighing the saponin content [23].

$$\% \, Weight \; of \; saponin = \frac{\text{weight of filter paper with residue} - \text{weight of filter paper}}{\text{Weight of sample analyzed}} \times 100$$

2.2.9 Gravimetric analysis

The pre-weighed aluminum sample was subjected to a gravimetric analysis in a controlled oven at 303, 313, and 323 K with immersion times of 2, 4, and 6 hours, respectively, and 0.5 M of NaOH solution in the presence or absence of OLE inhibitor concentrations of 0.3, 0.6, and 0.9 g/L. After removing the samples from the solution, acetone-cleaning them, and reweighing, the weight loss of each sample was ascertained. Weight loss was the outcome of the weight difference, which was found using Eq. (1). Using Eqs. (2) – (4) (ASTM G1 standard) and the weight loss data gathered, the following values were computed: the corrosion rate (CR), the inhibition efficiency (I.E%), and the degree of surface covering (θ):

$$W_2 - W_1, \qquad (1)$$

where W_1 is the weight before inhibition, and W_2 is the weight after inhibition

$$\mathrm{CR}\ (\frac{\mathrm{cm}}{\mathrm{hr}}) = \frac{87600\mathrm{W}}{\mathrm{A}\rho\ \mathrm{t}}, \quad (2)$$

where CR is the corrosion rate, w is the weight loss (g), A is the area of the coupon in (cm^2), t is time (h), and ρ is the density ($\mathrm{g/cm}^3$).

$$\mathrm{I.E}\ \% = 1 - \frac{\mathrm{CR_{inh}}}{\mathrm{CR_{blank}}} \times 100, \quad (3)$$

where I.E is the inhibition efficiency, with $\mathrm{CR_{inh}}$ and $\mathrm{CR_{blank}}$ corresponding to the corrosion rates in the presence and absence of inhibitors, respectively.

$$\theta = 1 - \frac{\mathrm{CR_{inh}}}{\mathrm{CR_{blank}}}, \quad (4)$$

where θ is the surface coverage, with $\mathrm{CR_{inh}}$ and $\mathrm{CR_{blank}}$ corresponding to the corrosion rates in the presence and absence of inhibitors, respectively.

2.3 Adsorption isotherm

The adsorption mechanism of organic inhibitors on the metal surface is described by means of adsorption isotherm investigations. According to [24], the adsorption isotherm model that most accurately depicts the adsorption of OLE on aluminum in 0.5 M of NaOH medium was created by fitting the inhibitor concentration (C) and the inhibitor's degree of surface coverage (θ) at 303 K for 2, 4, and 6 h immersion times into the Langmuir, Temkin, and Freundlich adsorption isotherm models expressed in linear form. [25].

$$\frac{\mathrm{C_{inh}}}{\theta} = \frac{1}{\mathrm{K_{ads}}} + \mathrm{C_{inh}} \quad (5)$$

$$\theta = \mathrm{K_{ads}} + \mathrm{In}\ \mathrm{C_{inh}} \quad (6)$$

$$\mathrm{Log}\ \theta = \mathrm{Log}\ \mathrm{K_{ads}} + \frac{1}{n}\mathrm{Log}\ \mathrm{C_{inh}} \quad (7)$$

Equation (8) establishes a relationship between the standard free energy of adsorption and the standard adsorption equilibrium constant of the inhibitor.

$$\Delta \mathrm{G_{ads}} = -\mathrm{RT}\ \ln(55.5\mathrm{K_{ads}}), \quad (8)$$

where R is the gas constant (8.314KJ/mol), T is the temperature (K), and 55.5 is the standard molar of water in the solution.

2.4 FTIR analysis

At Springboard Laboratory in Awka, an Infrared Spectrophotometer from Buck Scientific was used to perform FTIR analysis on OLE and the aluminum sample in the presence of OLE inhibitors. 0.5 g of KBr were used to prepare the samples. [26]. The sample was scanned within the wave number range of 600–4000 cm−1 in order to determine the functional groups and acquire the sample's spectra wavelength.

2.5 SEM analysis

Using a scanning electron microscope, the corroded coupons were analyzed morphologically. The aluminum sample's surfaces were examined using a scanning electron microscope in both uninhibited and OLE-inhibited basic media.

2.6 Electrochemical analysis

Using a computer-controlled potentiosta t/galvanostat, PDP and EIS curves were obtained in a traditional three-electrode cell. The reference electrode (RE) was Ag/AgCl in 3 M KCl, the counter electrode (CE) was platinum, and the working electrode (WE) was aluminum specimens. The WE's media-exposed area measured around 1 centimeter square. Prior to conducting potentiodynamic polarization (Tafel) studies, the electrode was left to corrode naturally for up to 12 minutes, which provided enough time for the electrode to reach a stable condition. [27]. The corrosion potential (Dcorr) of the working electrode was then found to be the steady-state OCP. Potentiodynamic measurements were conducted at 10 mVs−1 starting from the cathodic to the anodic direction (E = Dcorr ± 250 mV). Each sweep involved the employment of a new solution. The Echem Analyst software was used to analyze the PDP and EIS data. While the corrosion rate was assessed using Eq. (19), the inhibition efficiencies for PDP and EIS were computed using Eqs. (17) and (18) [28].

$$\mathrm{I.E\%_{PDP}} = \frac{\mathrm{icorr,0 - icorr}}{\mathrm{icorr,0}} \times 100 \quad (9)$$

$$\mathrm{I.E\%_{EIS}} = \frac{\mathrm{Rct - Rct,0}}{\mathrm{Rct}} \times 100 \quad (10)$$

$$\mathrm{C.R\ (mm/yr)} = 3.27 \times \mathrm{i_{corr}} \times \frac{\mathrm{e}}{\mathrm{p}}, \quad (11)$$

where Rct and Rct,0 represent the charge transfer resistance values for aluminum in 0.5 M NaOH when the inhibitor is present and absent, respectively. The symbols icorr,0, and icorr represent the inhibited corrosion current densities, respectively. e and ρ are the equivalent weight and density of aluminum, respectively, while 3.27 is the proportionality constant.

III. RESULTS AND DISUCSSION

3.1 An examination of phytochemical

Using both qualitative and quantitative methods, phytochemical analysis of OLE produced the following phytochemicals, which are reported in Tables 3 and 4.

Table 3 Qualitative Photochemistry Result

Inhibitor	Photochemical	Photochemical	Photochemical	Photochemical
	Alkaloid	Flavonoid	Saponin	Tannin
OLE	+	++	+++	++++

Phytochemicals are non-nutritive plant substances that have anti-inflammatory or disease-preventive properties. Flavonoids are secondary metabolites that are found in organic matter, such as plants and animals, and they may be beneficial to human health. Numerous antibacterial, antiviral, anti-inflammatory, anticancer, and anti-allergic properties have been demonstrated by studies on flavonoids [29]. Most oxidizing chemicals, such as singlet oxygen and different free radicals linked to a number of disorders, may be effectively scavenged by them [30]. Previous studies have demonstrated the potent immunomodulatory action of tannins [31]. Wound healing is caused by alkaloids because they contain a variety of pharmacological properties, such as antibacterial and anticancer properties [32]. Saponins are widely distributed in plants and are therefore considered to be phytochemical molecules that protect plants against illness [33]. The presence of these phytochemicals was thought to be responsible for the suppression of OLE-induced aluminum corrosion as the majority of them had chemical structures with heteroatoms or electron-rich linkages that made them more capable of donating electrons. [34].

Table 4. Quantitative Photochemistry Result

Inhibitor	Photochemical	Photochemical	Photochemical	Photochemical
	Alkaloid	Flavonoid	Saponin	Tannin
OLE	O.679%	0.659%	1.416%	7.578%

Table 5. GRAVIMETRIC ANALYSIS USING OLE

Time (h)	Inhibitor Conc. (g/L)	Wt. Difference (g)			Corrosion Rate (cm/h)			Inhibition Efficiency (%)			Degree of Surface Coverage (Θ)		
		Temperature (K)			Temperature (K)			Temperature (K)			Temperature (K)		
		303	313	323	303	313	323	303	313	323	303	313	323

2	BLANK 0.3 0.6 0.9	0.032 0.016 0.0042 0.0035	0.032 0.017 0.0072 0.005	0.037 0.019 0.009 0.0076	18.62 8.52 2.50 1.87	20.58 9.98 4.39 3.15	21.85 11.85 5.72 4.39	……..53.3287.6490.00	……..51.5878.7984.85	……..45.8475.2780.00	…….0.52210.87740.9000	……..0.51820.79900.8777	…….0.45820.74280.8000
4	BLANK 0.3 0.6 0.9	0.092 0.045 0.032 0.020	0.118 0.047 0.038 0.027	0.0130 0.078 0.039 0.026	28.02 12.48 9.39 6.24	36.52 14.02 10.92 7.49	40.28 23.75 11.89 8.14	……..56.5866.6777.81	…….61.5470.1880.00	…….42.0870.5980.02	……0.55560.67770.7781	……0.61850.70000.7948	…….0.41020.72550.8000
6	BLANK 0.3 0.6 0.9	0.168 0.075 0.055 0.038	0.179 0.083 0.059 0.0036	0.187 0.097 0.068 0.037	34.32 15.19 10.39 7.07	37.05 16.85 12.06 7.38	38.49 19.97 13.95 7.50	……..55.7869.	……...54.4968.	……..49.1063.	……0.55760.6	……0.55550.6	…….0.4900

								7279.39	4580.45	8280.59	9810.7948	7420.8123	0.64800.8123

3.2.1 Effect of inhibitor concentration

Table 4. displays the results of the gravimetric study, which indicate that as the concentration of Orange Leaf Extract (OLE) increases, so does the inhibition efficiency. Figure 2 illustrates this tendency. [35]. A protective coating that made it difficult for corrosive attack on the aluminum surface was created as a result of larger inhibitor molecules being absorbed at higher quantities on the aluminum surface when the concentration increased from 0.3g/L to 0.9g/L [36]. In a similar vein, the outcome demonstrates that greater inhibitory efficiency is implied by large surface coverage. The inhibition efficiency was completely blank when the inhibitor was not present.

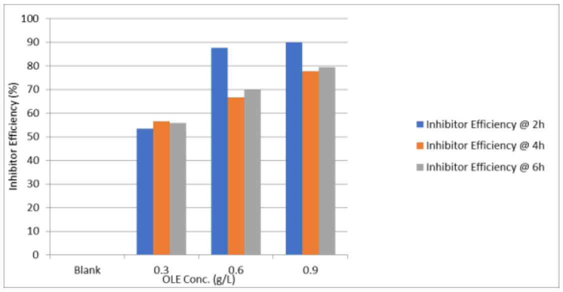

Fig 2. Effect of OLE concentration on Inhibitor efficiency using aluminum in 0.5M NaOH at a temperature of 303K

3.2.2 Effect of immersion time

The data in Tables 3 (F2) show that a longer immersion period at different doses of OLE inhibitors resulted in a higher corrosion rate and a lower inhibition efficacy. The inhibitory efficacy was observed to be decreased as a result of the phytochemical components' desorption from the metal surface, which increased the area exposed to the corrosive attack of sodium hydroxide. [37]. The strong inhibitory efficacy seen after immersion for two hours suggested that OLE inhibitors have been adsorbed to the aluminum surface in less than two hours. Consequently, the adsorbed effect of the inhibitor decreased with longer immersion times, whereas the mild activity of the basic media increased [38,39]. Resistance efficiency dropped as a result. Thus, inhibitor concentration is important in corrosion inhibition investigations.

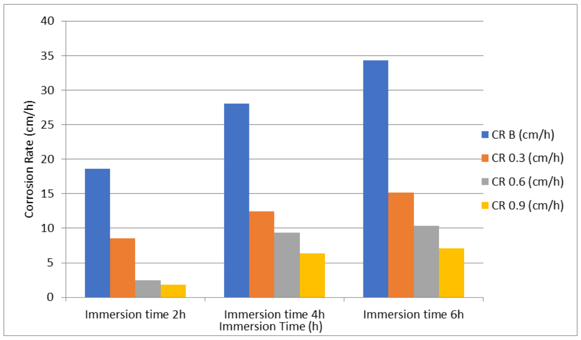

Fig. 3: Effect of immersion time on OLE corrosion rate of Aluminum in 0.5 NaOH with different inhibitor concentrations at a temperature of 303K

3.2.3 Effect of temperature

The data from Tables 4. show that as temperature climbed, the inhibition efficiency decreased and the rate of corrosion increased (Fig 3). This phenomenon happened because the OLE inhibitors' ability to adsorb on the aluminum surface was reduced, maybe as a result of the interacting molecules' higher average kinetic energy, which was aided by the higher temperature. Okewale and Adesina also observed that reaction rates generally increased with temperature (2020).

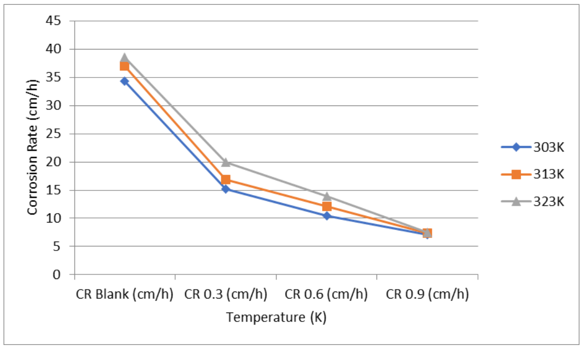

Fig. 4. Effect of temperature on OLE corrosion rate of Aluminum in 0.5 M NaOH with different inhibitor concentrations at 6h immersion time

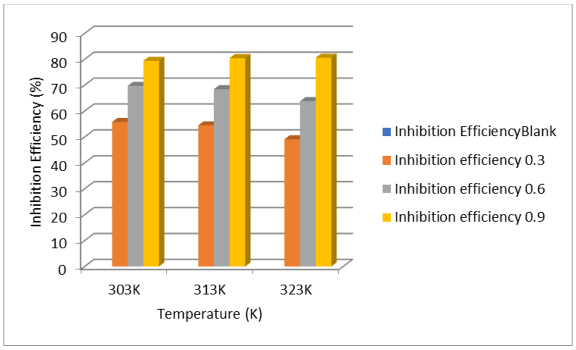

Fig. 5 Effect of temperature on Inhibition efficiency of Aluminum in 0.5 M NaOH with different inhibitor concentrations at 6h immersion time

3.2.4 Adsorption isotherm studies

The Langmuir, Freundlich, and Temkin adsorption isotherm models were fitted to the experimental data. The adsorption isotherm fitting outcomes are displayed in Figs. 4. 5, while Table 4. displays the adsorption isotherm parameters that were determined. With a correlation value (R2) of 0.947, the Temkin isotherm outperformed Freundlich and Langmuir in terms of fit for OLE inhibitors, according to the findings. The R2 values were nearly one, and the graphs showed good linearity. [40]. This suggests that the Temkin adsorption isotherm is strongly adhered to by the OLE inhibitors. According to the Temkin isotherm model, adsorption is characterized by a uniform distribution of binding energies up to a maximum binding energy, and the adsorption heat of every molecule present in the OLE decreases linearly with an increase in the coverage of the adsorbent surface [41]. According to the Temkin adsorption isotherm model, when the surface coverage of the adsorbent increases, the adsorption heat of the OLE molecules reduces linearly. This can be seen in Figure 4., where the surface coverage increases from 0.52 to 0.88 to 0.90.

Accordingly, the adsorption mechanism of the inhibitors on Aluminum in NaOH media is typical of physical adsorption, which involves electrostatic interaction between charged molecules. This is demonstrated by the adsorption of OLE inhibitors on the surface of Aluminum at the studied temperature with different immersion times [42].

Table 6. Adsorption Isotherm Parameters for OLE

Isotherm Models	Parameters	Inhibitor OLE
Langmuir	Intercept	0.49333
	Slope	0.5
	R^2	0.83678
	G_{ads}(kJ/mol)	-12.700
	R_L	0.2740
Freundich	Intercept	0.00884
	Slope	0.52103
	R^2	0.94616
	G_{ads}(kJ/mol)	12.380
Temkin	Intercept	0.98969
	Slope	0.36761
	R^2	0.94784
	G_{ads}(kJ/mol)	-9.205

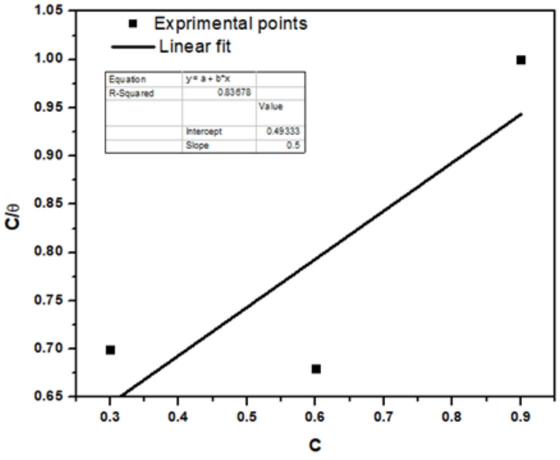

Fig. 6: Langmuir Isotherm model OLE

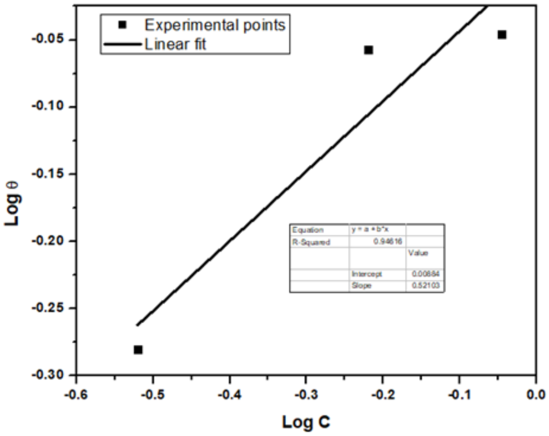

Fig. 7: Freundlich Isotherm model of OLE

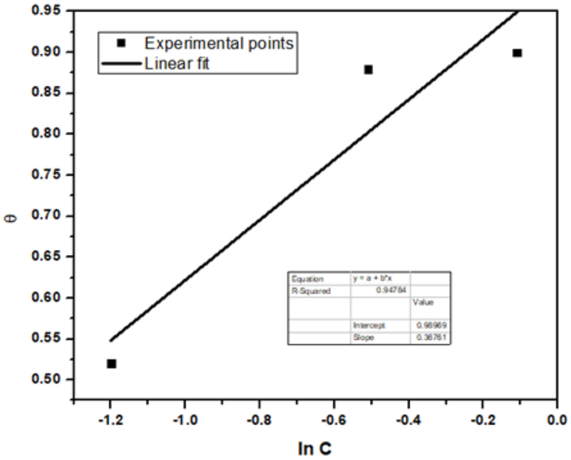

Fig. 8: Temkin Isotherm model of OLE

3.3 SEM Analysis

One useful method for characterizing the structure and composition of materials is SEM-EDX analysis. Scanning electron microscopy (SEM) in this study focuses on the sample's surface morphology, whereas electron dispersive X-ray spectroscopy (EDX) identifies the elements and their specific numbers, atomic concentrations, and weight concentrations.

3.3.1 SEM interpretation of blank aluminum

Eleven elements were identified through EDX analysis of blank aluminum metal, along with their individual element numbers, atomic concentrations (ppm), and weight concentrations (ppm), respectively. [43]. The morphology of the SEM image, observed in blank aluminum metal prior to corrosion inhibition, shows a distinctive irregular shape with a large parchment covering almost the surface area of the material with gray background.

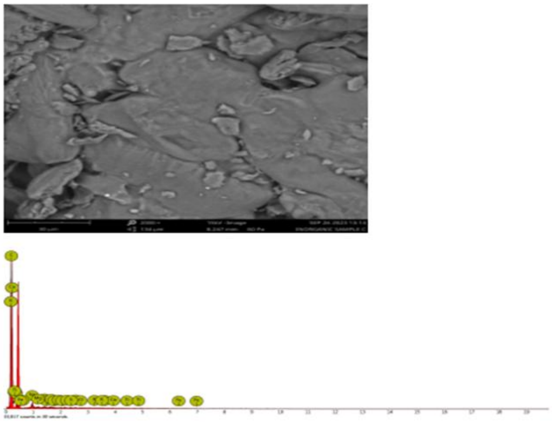

Fig 9: SEM-EDX Blank Aluminum Metal

Table 7: Table of EDX Analysis

Element Name	Element Number	Atomic Concentration (ppm)	Weight concentration (ppm)
Carbon	6	88.96	85.86
Nitrogen	7	0.24	0.52
Sodium	11	0.93	1.72
Aluminum	13	9.20	10.36
Magnesium	12	0.24	0.46
Silicon	14	0.17	0.38
Chlorine	17	0.10	0.30
Phosphorous	15	0.09	0.21
Sulfur	16	0.07	0.19
Calcium	20	0.00	0.00
Potassium	19	0.00	0.00
Titanium	22	0.00	0.00
Iron	26	0.00	0.00

	Total	100	100

The sample has a 100ppm atomic concentration of elements with carbon as the major element and a 100ppm weight concentration of elements with aluminum as the predominant element, according to an EDX examination of blank aluminum metal.

3.3.2 SEM interpretation of aluminum metal after inhibition

The morphology of the SEM image of the aluminum metal after inhibition displays a big, distinctive, irregularly shaped cut across the material's surface against a dark backdrop, indicating the presence of active sites for the inhibition of corrosion with orange leaf extract. Twelve elements were found in Aluminum Metal after inhibition by EDX analysis, along with information on each element's unique element number, atomic concentration (ppm), and weight concentration (ppm), respectively.

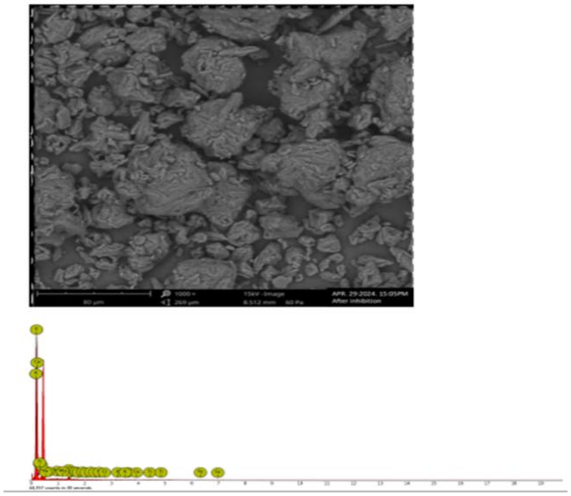

Fig 10: SEM-EDX Aluminum Metal after Inhibition

Table 8: Table of EDX Analysis

Element Name	Element Number	Atomic concentration (ppm)	Weight concentration (ppm)
Carbon	6	84.66	81.33
Nitrogen	7	14.12	15.82
Aluminium	13	0.39	0.83
Sodium	11	0.26	0.48
Iron	26	0.07	0.31
Magnessium	12	0.15	0.28
Silicon	14	0.10	0.22
Phosphorous	15	0.09	0.22
Sulphur	16	0.08	0.20
Chlorine	17	0.04	0.13
Calcium	20	0.03	0.09
Potassium	19	0.03	0.08
	Total	100.02	99.99

Following inhibition, an EDX analysis of aluminum metal reveals that the sample has an atomic concentration of 100.02 ppm and a weight concentration of 99.99 ppm, with the elements carbon and nitrogen predominating.

3.4 Fourier transform infrared (FTIR) analysis

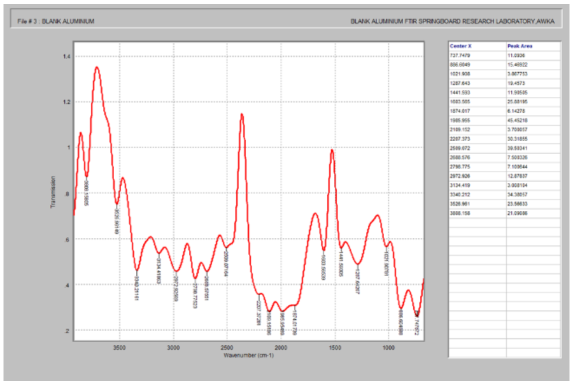

Fig 11 FTIR of Blank Aluminum metal before corrosion inhibition with OLE

Table 9: FTIR Interpretation of blank Aluminum metal before corrosion inhibition with OLE

Wavelength (cm^{-1})	Functional group	Compounds
886.6046	R-0-R	Ether C0 symmetric strech
1021.908	R-0-R	Ether C0 symmetric strech
1287.643	R-0-R	Ether C0 symmetric strech
1441.593	H_2C=CH	Ethene C=C anti-symmetric stretch
1603.565	RNH_3	1^0 amine NH stretch
1874.017	RNH_3	1^0 amine NH stretch
1985.955	SH	Thiol S-H symmetric stretch
2109.152	RC00H	Carboxylic acid C00 stretching vibration
2509.072	R-C≡N	Nitriles CN anti-symmetric stretch
2688.576	CH_2	Methylene CH symmetric stretch
2798.775	CH_2	Methylene CH symmetric stretch
2972.926	CH_2	Methylene CH symmetric stretch
3134.419	R_2CH0H	2^0 alcohols 0H symmetric stretch
3340.212	R_3CH0H	3^0 alcohols 0H symmetric stretch
3526.961	R_3CH0H	3^0 alcohols 0H symmetric stretch
3808.158	R_3CH0H	3^0 alcohols 0H symmetric stretch

An analytical method called Fourier Transform Infrared (FTIR) is used to examine organic functional groups and other substances that are present in a sample. In the current work, functional groups in the aluminum blank utilized for the corrosion inhibition investigation with extracted orange leaf extract were examined using Fourier transform infrared spectroscopy (FTIR). [44].The peak values near 1886.6046cm-1, 1021.908cm-1, and 1287.643cm-1 in the FTIR table above were attributed to the ester compound's C0 stretching vibration, respectively. Spectral height of approximately 1441.593cm-1 was attributed to the alkene compound's C=C anti-symmetric vibration. The N-H stretching vibration of the 10-amine compound was allocated to the medium band around 1603.565cm-1 and 1874.017cm-1, respectively. The peak height, which is approximately 1985.955 cm-1, is associated with the thiol compound's S-H stretching vibration. [45]. A wavelength of approximately 2109.152cm-1 was attributed to the carboxylic acid compound's C00 stretching vibration. The stretching vibration of CN in the nitrile compound was attributed to the highest value at approximately 2509.072cm-1. The C-H stretching vibration of the methylene molecule was identified as the source of the weak bands at 2688.576cm-1, 2798.775cm-1, and 2976.341cm-1, in that order. Strong bands were linked to the 0H stretching vibration of 20 and 30 alcoholic compounds, respectively, at 3134.419cm-1, 3340.212cm-1, 3526.961cm-1, and 3808.158cm-1.

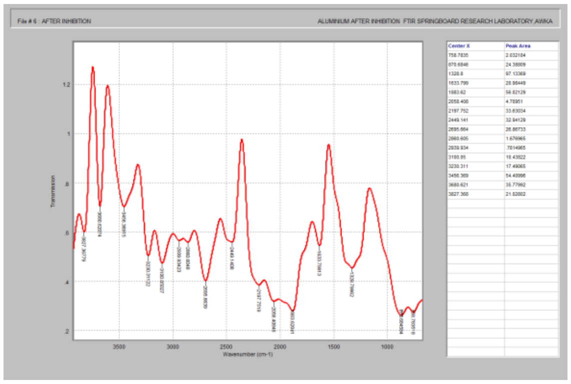

Center X	Peak Area
758.7835	2.032184
876.6846	24.38809
1328.8	97.13369
1633.799	28.98449
1883.62	56.82129
2058.408	4.78951
2197.752	33.63034
2449.141	32.94129
2695.664	26.86733
2860.605	1.679965
2939.934	.7814965
3100.05	18.43822
3230.311	17.49065
3456.369	54.40996
3680.621	35.77992
3827.368	21.82802

Fig 12 FTIR of Aluminum metal after Corrosion Inhibition with OLE

Table 10: FTIR Interpretation of Aluminium metal After Corrosion Inhibition with OLE

Wavelength (cm^{-1})	Functional group	Compounds
1328.800	$H_2C=CH$	Ethene C=C anti-symmetric stretch
1633.799	RNH_3	1^0 amine NH stretch
1883.620	RNH_3	1^0 amine NH stretch
2058.408	RC00H	Carboxylic acid C00 stretching vibration
2197.752	RC=0	Carbonyl compound C0 anti-symmetric stretch
2449.141	R-C≡N	Nitriles CN anti-symmetric stretch
2695.664	CH_2	Methylene CH symmetric stretch
2860.605	CH_2	Methylene CH symmetric stretch
2939.934	CH_2	Methylene CH symmetric stretch
3100.05	R_2CH0H	2^0 alcohols 0H symmetric stretch
3230.311	R_2CH0H	2^0 alcohols 0H symmetric stretch
3456.369	R_2NH	2^0 amine NH stretch
3680.621	R_3CH0H	2^0 alcohols 0H symmetric stretch
3827.368	R_3CH0H	3^0 alcohols 0H symmetric stretch

Based on the findings table, the absorbance at 1328.800cm-1 was attributed to the alkene compound's C=C anti-symmetric vibration. The N-H stretching vibrations of amine compounds 10 and 20 were allocated to the medium band around 1633.799cm-1, 1883.620cm-1, and 3456.369cm-1, respectively. [46]. The wavelength around 2197.752cm-1 was assigned to the C0 anti-symmetric vibration of the carbonyl compound, while the peak centered around 2058.408cm-1 was assigned to the C00 stretching vibration of the carboxylic acid compound. The peak value of 2449.141cm-1 was attributed to the nitrile compound's CN stretching vibration. The weak bands around 2695.664cm-1, 2860.605cm-1, and 2939.934cm-1 were identified as the methylene compound's C-H stretching vibrations, in that order. Strong bands at 3680.621cm-1, 3827.368cm-1, and 3100.05cm-1 were identified as the 0H stretching vibrations of alcohol compounds 10 and 30, respectively.

3.5 Electrochemical measurement studies

3.5.1. Open-circuit potential (OCP)

The potential created between the environment and the working electrode, which is the metallic surface under study, in relation to a reference electrode that will be put into the electrolyte near the working electrode, is known as the open circuit potential. [47]. The collected results showed that before the impedance and polarization experiments started, the solutions under investigation had acquired a satisfactory level of stability. The OCP value first varied at each concentration of OLE inhibitors before stabilizing (Fig. 4.14). The value of OCP increased in tandem with an increase in OLE concentrations. However, when the aluminum was added to 0.3 g/L of the OLE inhibitor, there was a discernible fluctuation that shifted in a negative direction throughout the course of the time. The value of OCP remained stable and was trending upward at OLE inhibitor concentrations of 0.6 and 0.9 g/L. This movement points to an OLE inhibitor's mixed-type corrosion inhibition action [48]. The OLE molecules' steady and unstable adsorption on the aluminum sample's surface could be the cause of the behavioral abnormalities. The adsorption isotherm, which demonstrates that it is also fitted to the Temkin isotherm model, is confirmed by this assertion of OLE molecules.

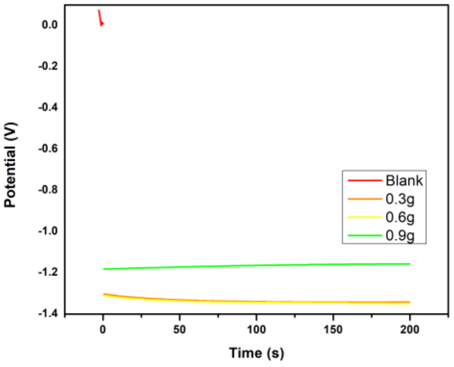

(a)

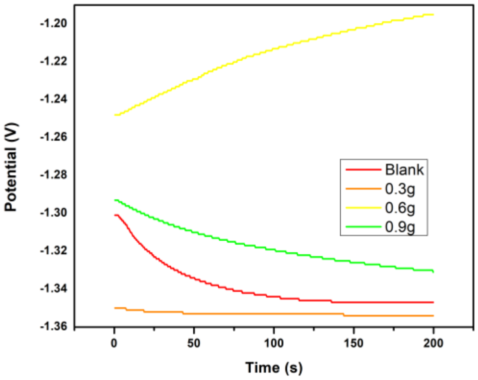

(b)

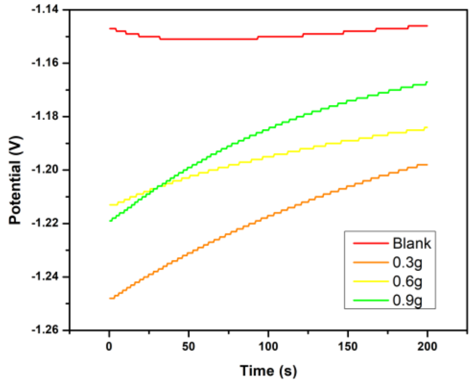

(c)

Fig 13: OCP curve for Aluminum in 0.5 NaOH OLE inhibitor at 303K for (a) 2h (b) 4h (c) 6h Immersion times

3.5.2 Electrochemical Impedance Spectroscopy (EIS)

With their corresponding Bode and phase angle representations displayed in figures (4.17 d, e, f) and (4.17 g, h, i), the Nyquist electrochemical plot of aluminum in 0.5M NaOH solution is shown in Figures (4.17 a, b, and c) in the presence and absence of increasing concentrations of OLE inhibitors at different immersion times.

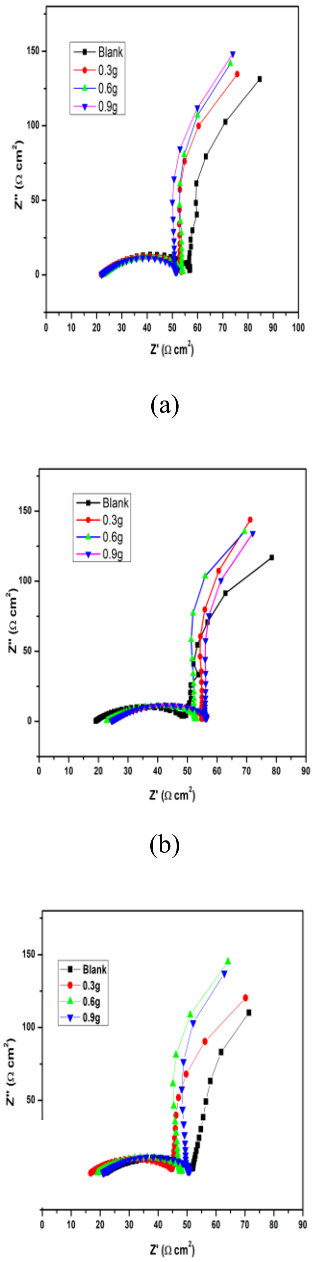

(a)

(b)

(c)

Fig.14 (a,b,c) Nyquist plots of Aluminum in 0.5M NaOH in the Absence and presence of different concentrations of OLE inhibitor at different immersion times

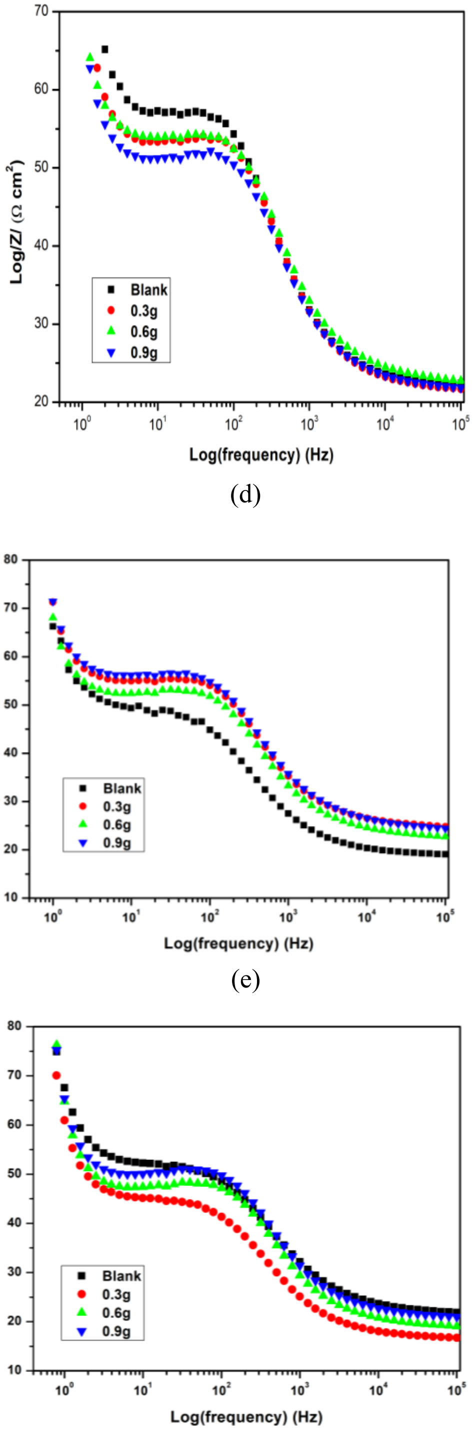

(d)

(e)

(f)

Fig 15 (d,e,f) Bode plots of Aluminum in 0.5M NaOH in the Absence and presence of different concentrations of OLE inhibitor at different immersion times

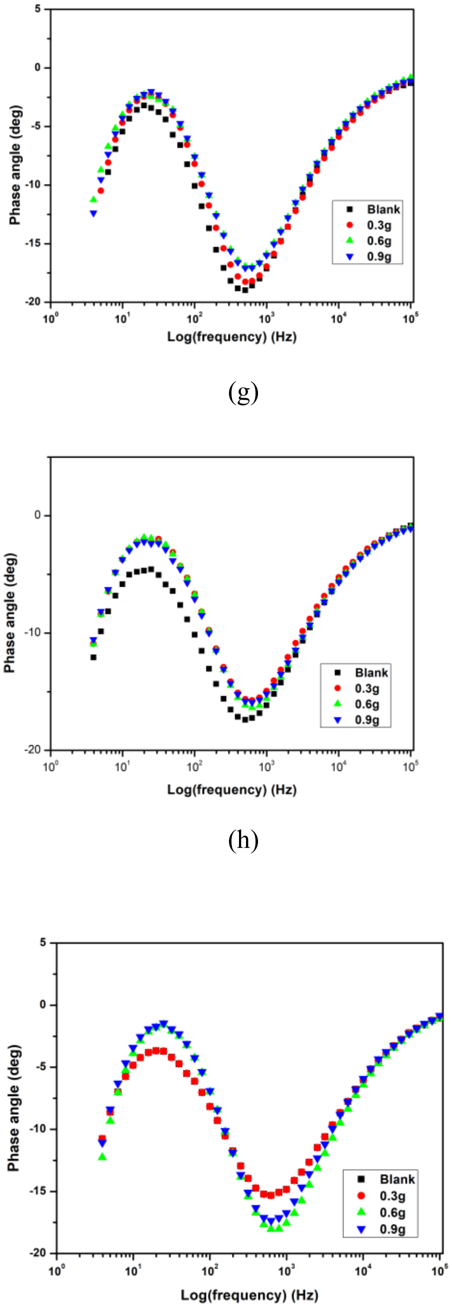

(g)

(h)

(i)

Fig 16 (g,h,i) Phase plots of Aluminum in 0.5M NaOH in the Absence and presence of different concentrations of OLE inhibitor at different immersion times

A similar semi-circle with a single, incomplete capacitive loop may be seen in the Nyquist plots of OLE inhibitors, suggesting a corrosion process controlled by charge transfer [49]. While the imperfections were brought about by various physical phenomena like roughness and heterogeneities on the working electrode surface, which could result from a corrosive attack on exposure to the acid solution, impurities, grain boundaries, and distribution of the surface-active sites, the shapes were similar because the corrosion mechanism remained unchanged [50]. The Nyquist plot width rose with the addition of OLE inhibitor at all doses, but this increase was most pronounced at 0.9 g/L for the inhibitor during all immersion times, indicating that the OLE inhibitor gave the aluminum greater corrosion resistance. The inhibitor's phase angle and Bode modulus graphs likewise showed this effect [51]. With increasing quantities of OLE and inhibitor, the phase angle was shown to be more negatively oriented, while the Bode modulus shifted in a noble direction. It may be inferred that the adsorption of OLE molecules on the aluminum surface slowed down the rate of charge transfer in the OLE inhibited system, reinforcing the protective barrier [52].

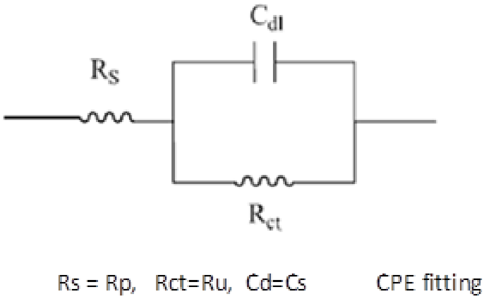

Fig. 17: The equivalent circuit diagram was employed to suit the data on impedance.

Fig. 4.15 displays the equivalent circuit that was utilized to fit the impedance values. The solution resistance (Rs) in the equivalent circuit is denoted by Rs, the charge transfer resistance (Rct) by Rf, the resistance of the adsorbed film's outer layer is described by Rf, and the constant phase element (CPE) of the inner and outer film layers (Y01 and Y02, respectively) by n1 and n2. Brug's formula [53]. can be used to compute the double-layer capacitance (Cdl) for a non-ideally polarized electrode, when charge transfer governs the corrosion process and diffusion is not taken into account.

$$C_{dl} = Y_0^{1/n} \left(\frac{1}{Rs} + \frac{1}{Rct}\right)^{n-1/n} \quad (21)$$

Tables 4.11 and 4.12 contain all of the derived values and calculated parameters. Based on the tables, an increase in OLE inhibitor concentration led to a corresponding rise in Rct values, which in turn produced an increase in inhibitor efficiency. Furthermore, for every immersion time under study, the Cdl values dropped. According to [54]. the higher Rct values further supported the theory that the slower rate of aluminum corrosion was to blame.

Table 11: Aluminum's electrochemical impedance characteristics in a 0.5M NaOH solution with and without an OLE inhibitor at various immersion durations

R_S (Ωcm^2)	R_{ct} (Ωcm^2)	n_1 (Ω)	Y_{01} ($\Omega^{-1}s^2cm^{-2}$)	R_f (Ωcm^2)	n_2 (Ω)	Y_{02} ($\Omega^{-1}s^2cm^{-2}$)	L (H)	IE (%)	C_{dl} (μFcm^{-2})
2 Hours									
33.81	23.8	0.925	1.33×10^{-5}	2.17×10^{-6}	0.457	2.83×10^{-7}	1.13×10^{-2}		6.31×10^{-6}
377.2	29.33	0.957	2.18×10^{-5}	1.137	0.964	2.26×10^{-3}	8.43×10^{-5}	18.85	1.286×10^{-5}
404	30.94	0.900	2.74×10^{-5}	2.804	1.00	2.78×10^{-3}	6.94×10^{-7}	23.08	7.78×10^{-6}
407.6	31.56	0.810	2.59×10^{-5}	3.221	1.00	2.69×10^{-3}	7.89×10^{-4}	24.58	2.56×10^{-6}
4 Hours									
446.2	18.44	0.913	2.78×10^{-5}	2.29×10^{-2}	2.47×10^{-2}	2.80×10^{-3}	9.75×10^{-2}		9.48×10^{-6}
28.53	20.64	0.920	3.52×10^{-5}	1.384	7.52×10^{-1}	1.62×10^{-5}	2.10×10^{-3}	10.66	1.218×10^{-7}
430.9	31.06	0.931	2.87×10^{-5}	1.000	7.31×10^{-1}	2.91×10^{-3}	2.73×10^{-3}	40.63	1.698×10^{-5}
437.7	38.98	0.915	2.92×10^{-5}	8.615	7.46×10^{-1}	2.89×10^{-3}	2.62×10^{-3}	52.69	1.023×10^{-5}
6 Hours									
28.05	23.73	0.930	3.10×10^{-7}	1.829	0.897	1.28×10^{-5}	4.58×10^{-6}		1.219×10^{-7}
26.31	28.16	0.938	3.32×10^{-7}	0.866	0.667	1.57×10^{-5}	8.36×10^{-5}	15.73	1.748×10^{-5}
434.5	30.36	0.901	2.68×10^{-5}	1.88	0.772	2.83×10^{-3}	9.97×10^{-10}	21.84	7.75×10^{-6}
437.7	35.78	0.960	2.87×10^{-5}	0.011	0.804	2.95×10^{-3}	5.10×10^{-7}	33.68	2.14×10^{-5}

3.5.3 Electrochemical measurements

Polarization via potentiodynamic electrochemical impedance and PDP Using a computer-controlled potentiostat /galvanostat, three conventional electrodes were used to construct spectroscopic EIS curves. The electrolyte resistance (Rs), the capacitance double layer (Cd), and the charge transfer resistance (Rct) are all measured using the EIS approach. Ag/AgCl in 3M KCl electrolyte was utilized as the reference electrode (RE), platinum electrode as the counter electrode (CE), and the sample as the working electrode (WE). The WE's exposed surface area to the media was roughly 1 cm2. When the medium was allowed to reach a stable condition at a constant open circuit potential without current flow, the sequential approaches were employed for the study. The AC signal is then scanned across a broad frequency range of 0.1 HZ to 10 KHZ to produce an impedance spectrum and to monitor the potentiodynamic polarization curve for the electrochemical cell that is being tested.

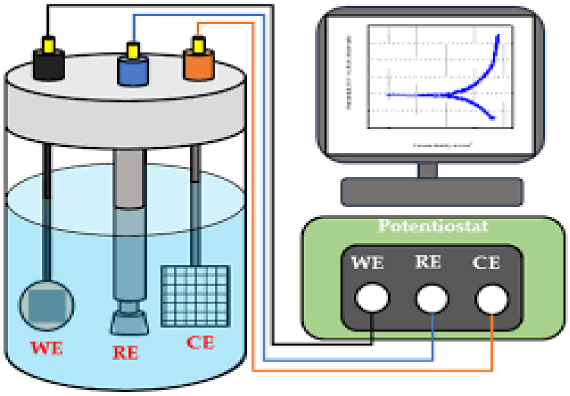

Fig 18: Electrochemical Corrosion Cell Setup

3.5.4 Potentiodynamic polarization (PDP)

In order to learn more about the kinetics of aluminum's anodic and cathodic processes, polarization experiments were carried out at 313 K for immersion times ranging from 2 to 6 hours in 0.5 M NaOH, both with and without OLE inhibitor. Figures 4.18 show the aluminum polarization curves at various OLE inhibitor doses and immersion periods. After analyzing the polarization curve, the appropriate parameters were determined through extrapolation, which included the corrosion potential (Ecorr), corrosion current density (icorr), and the anodic (βa) and cathodic (βc) Tafel slopes. The inhibition efficiency (η%) and corrosion rates of OLE inhibitor were calculated using equations 9 and 10, and the results are shown in Table 4.13 [55].

Table 12: Potentiodynamic polarization parameters of Aluminum in 0.5 M NaOH solution without and with different concentrations of OLE inhibitor at 313 K at 2, 4, and 6 h

2 Hours							
Inh. Con. (g/L)	E_{corr} (mV/SCE)	i_{corr} (mAcm^{-2})	β_a (mVdec^{-1})	$-\beta_c$ (mVdec^{-1})	CR (cm/hr)	η (%)	θ
Blank	-1.130	6.965×10^{-3}	406×10^{-3}	332.2×10^{-3}	1960		
0.3	-507.0	1.560×10^{-3}	215×10^{-3}	211.8×10^{-3}	712.9	63.38	0.6338
0.6	-508.0	1.25×10^{-3}	854.9×10^{-3}	738.5×10^{-3}	3771	82.02	0.8208
0.9	-495.0	1.15×10^{-3}	40×10^{-3}	42.20×10^{-3}	109.9	83.48	0.8348
4 Hours							
Blank	-1.340	8.67×10^{-3}	979.9×10^{-3}	593.7×10^{-3}	3.963×10^{-3}		
0.3	-1.350	1.250×10^{-3}	162.7×10^{-3}	123.6×10^{-3}	573.3	86	0.86
0.6	-1.330	1.140×10^{-3}	49.20×10^{-3}	44.60×10^{-3}	107.3	86.85	0.8685
0.9	-1.350	0.59×10^{-3}	568.1×10^{-3}	485.1×10^{-3}	2099	93	0.93
6 Hours							

Blank	-1.190	19.80×10^{-3}	395.1×10^{-3}	296.4×10^{-3}	9035		
0.3	-1.340	372×10^{-6}	52.20×10^{-3}	54.9×10^{-3}	124.2	98	0.98
0.6	-1.350	281×10^{-6}	41.60×10^{-3}	43.60×10^{-3}	82.83	98.50	0.9850
0.9	-1.160	260×10^{-6}	1.160	318.7×10^{-3}	2779	98.98	0.9898

The polarization curve demonstrates that the addition of OLE inhibitor repressed both the anodic and cathodic reactions, suggesting that OLE function as mixed-type inhibitors to inhibit the anodic dissolution and cathodic hydrogen evolution events. Tables 12 show that the addition of OLE inhibitor with the highest displacement at 6 hours of immersion time resulted in a corrosion potential (Ecorr) of 15 mV as compared to the blank acid solution. The fact that the Ecorr value is less than 85 mV indicates that OLE inhibitors function as mixed-type inhibitors, regulating the anode and cathode's corrosion reaction [56]. Additionally, the values of the corrosion potential and corrosion current density gradually decrease as the inhibitor concentration rises. As a result, the anodic and cathodic inhibition performances block the active sites on the aluminum surface, increasing inhibition efficiency and lowering corrosion rates. The OLE molecules were adsorbed by the aluminum during all immersion times, resulting in this effect. With an inhibitor concentration of 0.9 g/L, the OLE's inhibition efficiency peaked at 6 hours of immersion time, or 98.98%. The same tables demonstrate that for both inhibitors, the change in the anodic Tafel slope (βa) is greater than the shift in the cathodic Tafel slope (βc) when compared to the blank. This suggests that the anodic reaction is mostly affected by OLE inhibitors [57, 58].

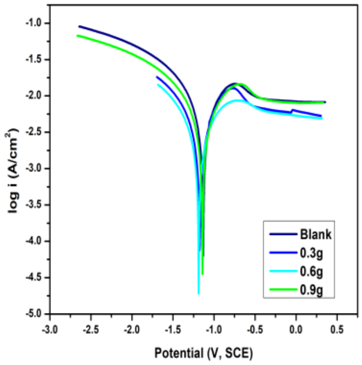

(a)

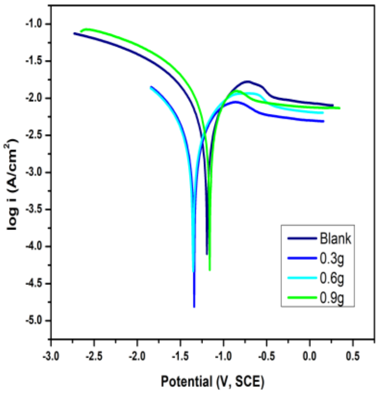

(b)

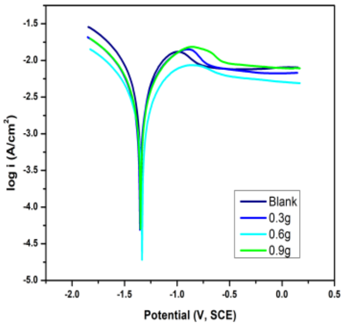

(c)

Fig. 19: Polarization curves of Aluminum in 0.5 M NaOH with different concentrations of OLE inhibitor at 303 K for (a) 2h (b) 4h (c) 6h immersion time

CONCLUSION

It is thought that a large number of studies have mostly concentrated on the use of extremely basic or acidic substances for corrosion inhibition; however, some studies have also focused on plant extract, and a small number have taken biological products into consideration. The objective of this research was to create and examine a novel inhibitor system and evaluate its efficacy in inhibiting metal corrosion. Orange leaf extract was investigated since it is an organic material and may be able to prevent aluminum from corroding in basic conditions. Our examination included the use of potentiodynamic polarization, electrochemical impedance spectroscopy, scanning electron microscopy, FTIR analysis, including adsorption, and weight loss. The findings led to the following deductions being made: According to the results of the phytochemical investigation, the presence of phenolic agents and metabolites was responsible for the inhibitive activities of OLE. Alkaloids, flavonoids, saponin, and tannin were also found. The aluminum samples' surface developed a barrier thanks to the action of these phenolic compounds and metabolites.

According to the gravimetric analysis, the OLE inhibitor's aluminum inhibition efficacy rose as inhibitor concentration rose but fell as temperature and time increased. 90% was the maximum OLE inhibitor inhibition efficiency, achieved at 0.9 g/L for 2 hours at 303 K. Aluminum will therefore corrode in NaOH at a different rate depending on the temperature, concentration, and immersion period. The Langmuir adsorption isotherm model was in agreement with the OLE inhibitor's adsorption mechanism. The inhibitor was typical physisorption because the adsorption-free energy ΔG^o ads, which showed a negative value, suggested that the OLE inhibitor adsorbs spontaneously on aluminum. An increase in half-life values in tandem with a drop in the rate constant suggested that the OLE inhibitor is an effective inhibitor for the system under investigation. OLE's inhibition was found to be actively caused by the functional groups O–H, C–H, C–CI, C = C, C–N, COOH, and N–H, according to Fourier Transform Infrared (FTIR) Spectroscopy. Analyses using scanning electron microscopy (SEM) revealed that the phenolic agent/metabolite molecules' adsorption on the metal surfaces resulted in the creation of a protective coating on the aluminum samples' surfaces, which mitigated corrosion. The OLE inhibitor's phase, Nyquist, Bode, and electrochemical impedance spectroscopy (EIS) plots showed that charge transfer governs the corrosion process. While the Cdl values fell for all of the investigated immersion times, the rise in inhibitor concentrations led to an increase in both the Rct values and inhibitor efficiency. This implies that the inhibitors' molecules have adhered to the metal surface. At a 4-hour immersion duration, OLE's corrosion inhibition efficiency was 88.9%, according to the potentiodynamic polarization (PDP) result. OLE inhibitor demonstrated that it functioned as a mixed-type inhibitor by interfering with both the anodic and cathodic processes.

REFERENCES

[1] Adegbite, J. A., Sanni, L. O., Osinowo, O. A. (2006). *Comparative evaluation of chemical and sensory properties of Achatina achantina and Archachatina marginata. International Journal*. Asset Series A, 6 (2):1–6.

[2] Aiawadhi, K., Robinson, M., Chalmers, A., & Winning, I. G. (2008). *Inhibition of weld corrosion in flowing brines containing carbon dioxide. NACE* - International Corrosion Conference Series, 086221–0862214.

[3] Akintayo Rotibi, Kunle Adesina and Segun Michael Abegunde. Raphia *taedigera seed extract as a green corrosion inhibitor for the corrosion of mild steel in acidic media*. World Journal of Advanced Engineering Technology and Sciences, 2022, 06(01), 040–046. DOI: https://doi.org/10.30574/wjaets.2022.6.1.0063

[4] Ameh P.O, Ukoha P, Ejikeme P, Eddy NO (2016). *Thermodynamic, Chemical and Electrochemical Investigations of 4-Hydrobenzoic Acid as Corrosion Inhibitor for Mild Steel Corrosion in Hydrochloric Acid Solutions*. Ind Chem 2: 119. DOI: https://doi.org/10.4172/2469-9764.1000119

[5] *Aschoff, Julian K.; Kaufmann, Sabrina; Kalkan, Onur; Neidhart, Sybille; Carle, Reinhold; Schweiggert, Ralf M. (2015-01-21). "In Vitro Bioaccessibility of Carotenoids, Flavonoids, and Vitamin C from Differently Processed Oranges and Orange Juices [Citrus sinensis (L.) Osbeck]". Journal of Agricultural and Food Chemistry. 63 (2): 578–587. doi:10.1021/jf505297t. ISSN 0021-8561.*

[6] Ashraf, A., Sarfraz, R.A., Rashid, M.A., Mahmood, A., Shahid, M. Noor, N. *Chemical composition, antioxidant, antitumor, anticancer, and cytotoxic effects of Psidium guajava leaf extracts*. Pharm. Biol. 2016, 54, 1971–1981.

[7] Awe I. Caroline., Abdulrahaman A. S., Ibrahim H. Kobe, Kareem A. Ganiyu, & Adams S. M., (2015). Inhibitive Performance of Bitter Leaf Root Extract on Mild Steel Corrosion in mn Sulphuric Acid Solution. American Journal of Materials Engineering and Technology. 3(2):35–45.

[8] *Bai, Jinhe; Baldwin, Elizabeth B.; Hearn, Jake; Driggers, Randy; Stover, Ed (2014). "Volatile Profile Comparison of USDA Sweet Orange-like Hybrids versus 'Hamlin' and 'Ambersweet'".HortScience. 49 (10): 1262–1267. doi:10.21273/HORTSCI.49.10.1262. Archived from the original on 2016-07-21. Retrieved 2018-03-18*

[9] Bhosale U.A, Yeganarayan R, Pophale P, Somani R. *Effect of aqueous extracts of Achyranthes Aspera Linn. On an experimental animal model for inflammation*. Ancient Science of Life. 2012;31(4):202

[10] Boffarh B.P. *Corrosion Inhibitors in the Water Treatment Industry in ASM Handbook*, Vol 13A, ASM International; Materials Park OH (2003).

[11] *Boltres, Bettine (2015). When Glass Meets Pharma: Insights about Glass as Primary Packaging Material. Editio Cantor. ISBN 978-3-87193-432-2.*

[12] Brug, G.J., van den Eeden, A.L.G., Sluyters-Rehbach, M., Sluyters, J.H.,. *The analysis of electrode impedances is complicated by the presence of a constant phase element. J. Electroanal. Chem.* 176, 275–295, 1984. Https://doi.org/10.1016/S0022-0728(84)80324-1.

[13] Chen, H.Y.; Yen, G.C. *Antioxidant activity and free radical-scavenging capacity of extracts from guava (Psidium guajava L.) Leaves.* Food Chem. 2007, 101, 686–694.

[14] *Daniel Robles. "Potable Water Pipe Condition Assessment For a High Rise Condominium in The Pacific Northwest". GSG Group, Inc. Dan Robles, PE. Archived from the original on 29 December 2017. Retrieved 10 December 2012.*

[15] Daniel. *The preparation and characterization of chitosan membrane derived from shrimp shell of Mahakam River*, Mulawarman Scientific Journal, 8, (1):39–49 (2009).

[16] Dereje A. Oncho, Meseret C. Ejigu and Olyad E. Urgessa. *Phytochemical constituent and antimicrobial properties of guava extracts* of east Hararghe of Oromia, Ethiopia. Clinical Phytoscience (2021) 7:37 https://doi.org/10.1186/s40816-021-00268-2

[17] Dewi, P.S.; Sutjiatmo, A.B.; Nurdiansyah, A. *Antidiarrheal activity of water extracts of guava leaves (Psidium guajava L.) And water extracts of green tea leaves (Camellia sinensis L.) Combination in Swiss Webster mice.* Acta Pharm. Indones. 2013, 38, 67–70.

[18] Evaluation, I., Chemical, O. F., Extracts, P., The, O. N., Of, C., Alloys, M., & Acidic, I. N. (2016). *Inhibition evaluation of chemical and plant extracts on the corrosion of metallic alloys in an acidic environment.*

[19] Evans, W.C., (2006). *Pharmacognosy,* 16th Edition, W.B. Sounders, USA. Pp. 243-283.

[20] Falah, S. A., Saja, N. M. (2017). *Essential Trace Elements and Their Vital Roles in Human Body, Indian Journal of Advances in Chemical Science*, 5 (3):127–136.

[21] Farag, R.S.; Abdel-Latif, M.S.; Abd El Baky, H.H.; Tawfeek, L.S. *Phytochemical screening and antioxidant activity of some medicinal plants' crude juices.* Biotechnol. Rep. 2020, 28, e00536.

[22] Fontana M.G, Greener N.D, (1978). *The Eight Forms of Corrosion, Corrosion Engineering*, MG-Graw-Hill, New York

[23] Frank N.K, and John MC, (1979). *The Nalco Water Handbook*. Griffiths, P.; de Hasseth, J. A. (18 May 2007). *Fourier Transform Infrared Spectrometry* (2nd ed.). Wiley-Blackwell. ISBN 978-0-471-19404-0

[24] Harti, A.S, Sulisetyawati, D., Murharyati, A., Oktariani, M. (2016). *The Effectiveness of Snail Slime and Chitosan in Wound Healing, International Journal of Pharma Medicine and Biological Sciences, 5: 1–5.*

[25] Hassan SB, Gulbo J, Hu K, Berenjian S, Morein B, Nygren P. *The Nanoparticle Quillaja Saponin BBE is selectivity active towards renal cell carcinoma.* Anticancer Res 2013;33(1):143-51

[26] *Hoffman, Robert S.; Burns, Michele M.; Gosselin, Sophie (2020). "Ingestion of Caustic Substances". New England Journal of Medicine. 382 (18): 1739–1748. doi:10.1056/nejmra1810769. PMID 32348645.*

[27] Izionworu, V. O., Ukpaka, C. P., & Oguzie, E. (2020). *Green and eco-benign corrosion inhibition agents Alternatives and options to chemical-based toxic corrosion inhibitors Green and eco-benign corrosion inhibition agents: Alternatives and options to chemical-based toxic corrosion inhibitors.* Https://doi.org/10.5281/zenodo.3706592.

[28] J. T. Nwabanne, V. N. Okafor, *Adsorption and thermodynamics study of the inhibition of corrosion of mild steel in H_2SO_4 medium using Vernonia amygdalina, J. Minerals Mater*. Characteri. Eng., 11, (2012), 885-890.

[29] Jamiu K., Odusote, David O., Owalude, Sunday J., Olusegun, & Raheem A. Yahya, (2016). *Inhibition Efficiency of Moringa oleifera Leaf extracts on the Corrosion of Reinforced Steel Bar in Hcl Solution*. The West India J. Of Engineering. 38(2):6470.

[30] JE Breakell, M Siegwart, K Foster, D Marshall, M Hodgson, R Cottis, S Lyon (2005). *Management of Accelerated Low Water Corrosion in Steel Maritime Structures*, Volume 634 of CIRIA Series, ISBN 0-86017-634-7

[31] Jiang, L.; Lu, J.; Qin, Y.; Jiang, W.; Wang, Y. *Antitumor effect of guava leaves on lung cancer: A network pharmacology study*. Arab. J. Chem. 2020, 13, 7773–7797.

[32] *Jones, Denny A. (1991). Principles and prevention of corrosion. New York : Toronto : New York: Macmillan Pub. Co. ; Collier Macmillan Canada ; Maxwell Macmillan International Pub. Group. ISBN 978-0-02-361215-2.*

[33] K. T. Dauda, V. N. Atasie, and A. A. Adetimilehin. *Kinetics of the Inhibitory Effects of Ethanolic Extract of Vernonia amydgalina on the Corrosion of Aluminium in 1.0 M hcl*. Chem. J., 3, (2013), 86-89

[34] Kavitha N., Manjula P., & Anandha kumar N., (2014). *Synergistic Effect of Papaya Leaves Extract Zn^{2+} in Corrosion Inhibition of Mild Steel in Aqueous Medium*. Research Journal of Chemical Sciences. 4(8):88–93.

[35] *Koch, Gerhardus H.; Brongers, Michiel P.H.; Thompson, Neil G.; Virmani, Y. Paul; Payer, Joe H. (September 2001). "Corrosion costs and preventive strategies in the United States". CC Technologies Laboratories, Inc. Federal Highway Administration (FHWA). Archived from the original on 2011-07-08.*

[36] Kolawole S. Amoo, Jacob S. Jatau, M. Abdulwahab. *Corrosion Inhibitive Effect of Psidium Guajava Leaves on Mild Steel in an Induced Alkaline Solution*. Journal of Scientific and Engineering Research, 2019, 6(6):116-127

[37] Laily, N.; Kusumaningtyas, R.W.; Sukarti, I.; Rini, M.R.D.K. *The potency of guava Psidium guajava (L.) Leaves as a functional immunostimulatory ingredient*. Procedia Chem. 2015, 14, 301–307.

[38] Leelavathi S., & Rajalakshmi R., (2013). *Dodonaea viscose (L.) Leaves Extract as an acid Corrosion Inhibitor for Mild Steel.* Journal of Material and Environment Science. Vol. 4(5), pp 625–638.

[39] Manoj Kumar, Maharishi Tomar, Ryszard Amarowicz, Vivek Saurabh, M. Sneha Nair, Chirag Maheshwari, Minnu Sasi, Uma Prajapati, Muzaffar Hasan, Surinder Singh, Sushil Changan, Rakesh Kumar Prajapat, Mukesh K. Berwal and Varsha Satankar. Foods 2021, 10, 752. https://doi.org/10.3390/foods10040752

[40] Mazumdar, S.; Akter, R.; Talukder, D. *Antidiabetic and antidiarrhoeal effects on*

ethanolic extract of Psidium guajava (L.) Bat. Leaves in Wister rats. Asian Pac. J. Trop. Biomed. 2015, 5, 10–14.

[41] Miralrio, A., & Vázquez, A. E. (2020). *Plant extracts as green corrosion inhibitors for different metal surfaces and corrosive media*: A review. Processes, *8*(8). Https://doi.org/10.3390/PR8080942

[42] *Morton, Julia F. (1987). Fruits of Warm Climates. pp. 134–142. Archived from the original on 2019-05-26. Retrieved 2020-05-05.*

[43] Moses M. Solomon, Saviour A. Umoren, Mumtaz A. Quraishi, Divya B. Tripathy, Ekaette J. Abai. *Effect of alkyl chain length, flow, and temperature on the corrosion inhibition of carbon steel in a simulated acidizing environment by an imidazoline-based inhibitor*. Journal of Petroleum Science and Engineering 187 (2020) 106801. Https://doi.org/10.1016/j.petrol.2019.106801

[44] Naoshi, K., Yasusato, S., Masakichi, S., Kawakita, M. (2005). *The preparation of Chito-oligosaccharides by two-step hydrolysis*, Chitin and Chitosan Research, 11 (2): 170–171.

[45] *Nicolosi, E.; Deng, Z. N.; Gentile, A.; La Malfa, S.; Continella, G.; Tribulato, E. (2000). "Citrus phylogeny and genetic origin of important species as investigated by molecular markers". Theoretical and Applied Genetics. 100 (8): 1155–1166. doi:10.1007/s001220051419. S2CID 24057066.*

[46] Noyel Victoria S., Rohith Prasad, & Manivannan R. (2015). *Psidium Guajava Leaf Extract as Green Corrosion Inhibitor for Mild steel in Phosphoric Acid*. Int. J. Electrochem. Sci. 2220–2238

[47] *Nwagha, Nzube. "Statistical study on the corrosion of mild steel in saline mediums".*

[48] Okewale, A.O; Adesina, O.A. *Kinetics and Thermodynamic Study of Corrosion Inhibition of Mild Steel in 1.5M HCl Medium using Cocoa Leaf Extract as Inhibitor*. J. Appl. Sci. Environ. Manage. Vol. 24 (1) 37-47 January 2020. DOI: https://dx.doi.org/10.4314/jasem.v24i1.6

[49] *Paterson, Ian (2003). A Dictionary of Colour: A Lexicon of the Language of Colour (1st paperback ed.). London: Thorogood (published 2004). p. 280. ISBN 978-1-85418-375-0. OCLC 60411025.*

[50] Perez, W.P., Dina, F., Iwang, Y. (2012). *Effect of mucus snail (Achatina Fulica) against total cells fibroblasts on incision wound healing skin of mice (Mus musculus)*, Journal of Veterinary Medical Science and Health, 4 (2): 195–203.

[51] Piccin J.S, Dotto G.L. and Pinto L.A.A *Adsorption Isotherm and Thermochemical Data of FD&C Red N◦40 Binding* By Chitosan

[52] Priya Bhardwaj, 2017. *"studies on potential green corrosion inhibitors for mild steel in different media."*

[53] Putilora I, Balezin S, Barannik V, (1960). *Metalic Corrosion Inhibitors, G. Ryback Translator,* Pergamon Press, New York.

[54] Rajeswari A. *Evaluation of phytochemical constituents, quantitative analysis and antimicrobial efficacy of potential herbs against selected microbes*. Asian J Pharm Clin Res 2015;8(2)'232-7

[55] *R. Zuo; D. Örnek; B.C. Syrett; R.M. Green; C.-H. Hsu; F.B. Mansfeld; T.K. Wood (2004). "Inhibiting mild steel corrosion from sulfate-reducing bacteria using antimicrobial-producing biofilms in Three-Mile-Island process water". Appl. Microbiol. Biotechnol. 64 (2): 275–283. doi:10.1007/s00253-003-1403-7. PMID 12898064. S2CID 20734181.*

[56] Saedah R. Al-Mhyawi. *Inhibition of mild steel corrosion using Juniperus plants as green inhibition. African Journal of Pure and Applied Chemistry*. Vol. 8(1), pp. 9-22, January, 2014. DOI:10.5897/AJPAC2013. 0497

[57] Sani L.M, Abdulwahab M., Yaro S. A., & Umaru O. B., (2015). *Inhibitive Effect by Psidium guajava Leaf Extract on the Corrosion of Al-Si-Mg (SSM-HPDC) Alloy in Simulated Sea water Environment*. Metall. Mater. Eng. 21(4):241-251

[58] *Schweitzer, Philip A. (2010). Fundamentals of corrosion – Mechanisms, Causes and Preventative Methods. Taylor and Francis Group. p. 25. ISBN 978-1-4200-6770-5.*

[59] Siaka A. Abdulfatai, Owa. O Sunday, M. K. Gafar, and J O. Okunola. *Corrosion inhibition efficiency, adsorption behavior, kinetics and*

thermodynamic studies of lannea acida ethanol leaves extract on mild steel in hydrochloric acid. Vol. 5 No. 2, June 2021, pp 621-634 DOI: https://doi.org/10.33003/fjs-2021-0502-678